28th EUROPEAN ROTORCRAFT FORUM

Session Dynamics 7
Paper 89

Full Scale Rotor with Piezoelectric Actuated Blade Flaps

by

Bernhard Enenkl
Valentin Klöppel
Dieter Preißler

EUROCOPTER Deutschland GmbH, Munich, Germany

Peter Jänker

EADS Corp. Research Center, Munich, Germany

SEPTEMBER 17 - 19, 2002
BRISTOL
UNITED KINGDOM

FULL SCALE ROTOR WITH PIEZOELECTRIC ACTUATED BLADE FLAPS

Bernhard Enenkl
Valentin Klöppel
Dieter Preißler
EUROCOPTER Deutschland GmbH, Munich, Germany

Peter Jänker
EADS Corp. Research Center, Munich, Germany

Abstract

Flight testing of a main rotor with controlled trailing edge flaps is the aim of a research project called ADASYS, a joint task between Eurocopter, EADS CRC, DaimlerChrysler Research Labs, and DLR in Germany.

This paper reviews the development of a full scale rotor based on the hingeless system of the BK117/EC145. The pre-design phase dealt with the definition of the flap dimensions and its radial location on the blade for an efficient use for vibration suppression and noise reduction. A piezoelectric actuator concept (EADS CRC) seems to be adequate for installation in the rough environment of a helicopter rotor blade. Wind tunnel and centrifugal tests confirmed the approach.

Recent activities concentrated on the design and construction of the rotor blades as well as on the bench testing of key components. The whirl tower test confirmed the dynamic lay-out and the aerodynamic efficiency of the flaps being now ready for flight.

The flight test campaign will be based on the individual blade root control (IBC) tests on the BO105 helicopter during recent years [1]. For the flight tests with controlled trailing edge flaps fon BK117 DaimlerChrysler Research Labs developed an optical data link and a brushless electrical power transmission between airframe and rotating system as well as the power amplifiers supplying the piezoelectric actuators.

The programme is supported by the German Ministry of Economics (BMWi).

Notations

ATR	Advanced technology rotor
BVI	Blade vortex interaction
R	Rotor radius
rev	Revolution

Presented at the 28th European Rotorcraft Forum, 17. - 19. September 2002, Bristol, UK

Introduction

The public acceptance of today's helicopters still suffers from several deficiencies. One is the annoying exterior impulsive noise emission, also known as Blade Vortex Interaction Noise – BVI Noise. Another is the high cabin vibration level compared to airliners. Further challenges are the blade lead-lag damping and stall at high cruise speeds and load factors. As a powerful palliative against all these phenomena the Active Blade Control – ABC is widely accepted [2]. This control is superimposed to the pilot's flight control inputs. It is accomplished by actuators in the rotating system and is mostly but not necessarily harmonic with respect to the rotation of the rotor.

Fig. 1 EC145 full scale rotor blade with piezoelectric actuated trailing edge flaps

There are actually two technical solutions under test. One is the blade pitch control at the blade root, usually called Individual Blade Control – IBC. It replaces the rotating control rods between swash plate and blade pitch horn by an actuator of high bandwidth [3]. The second is the blade pitch control by servo flaps at the blade's outer trailing edge shown in Fig. 1.

ECD cooperates with ZFL since many years in the development of IBC [3], [4]. It applies this control method actually for development and test of ABC control algorithms [5]. The main effort of the development of a future ABC system is however

focused on the servo flap control as a first step towards a distributed actuation system as well towards a replacement of the swash plate. Hence, flap control will be the subject of this presentation.

The control input may range from steady to about 6/rev (i.e. six sinusoidal periods per rotor revolution) depending on application goal and blade number.

A steady input is required for automatic rotor tracking and compensation of rotor unbalances over the flight envelope. For BVI noise suppression and stall delay at the retreating blade, a 2/rev input is appropriate. Vibration excitation of four-bladed rotors is tackled by 3/rev, 4/rev and 5/rev control. Shocks on the advancing blade, leading to high speed impulsive noise and advancing blade stall are expected to be destabilised by inputs above 5/rev. This frequency range is also applied for the delaying of stall flutter onset.

The control amplitude required is expected for all applications with the exception of retreating blade stall delay below 1,5° pitch. This is of utmost importance, since this control authority is moderate enough that control failures such as blockings or run-aways can be tolerated. Only a fixing or an inherent stiffness of the actuator in case of power loss must be assured.

The flaps are driven by piezoceramic actuators with mechanical stroke amplification. The advantage of this system is first the electric power supply which allows a favourable transmission from the fixed into the rotating system, then, the lack of wear, friction and play, robustness and small volume, and finally the inherent stiffness mentioned above. Efficiency and endurance of piezoceramics have made considerable progress in the last years [6], [7]. Nevertheless, up to now, besides first whirl tower tests [8], no far-reaching full scale application of active flaps has been realized.

Concept Decision

Rotor Characteristics

Table 1 Advanced Technology Rotor (ATR) characteristics

Aircraft	BK117 - EC145
Airfoil	OA series
Twist	12 deg
System	Hingeless
Rotor radius	5.5 m
Equivalent chord	0.325 m
Tip speed	221 m/sec
Torsion frequency	4.3/rev

During the concept decision phase, rotor blades developed within the Advanced Technology Rotor (ATR) research project [9] were taken as baseline for the investigations. This is a four-bladed hingeless rotor system with removable blade tips which fits the BK117 helicopter. The planform has inboard tapering and features a sweptback parabolic tip. Table 1 shows the blade main parameters.

Flap Location and Dimensions

The way how trailing edge flaps reduce noise and vibration may vary, depending mainly on flap chord, control frequency, and the blade's torsional stiffness. Larger flap chords and high torsional blade stiffness lead rather to a direct lift effect by flap deflections. On the contrary, smaller flap chords and lower torsional blade stiffness support rather the flap's servo effect in form of a blade pitching moment. For lower control frequencies, both effects are counteracting. For control frequencies above the first torsional eigenfrequency both effects act in the same direction.

Another important parameter is the radial position of the flap. A parametric study with the rotor code CAMRAD II based on the ATR properties revealed that for BVI noise reduction purposes, the flap should be shifted as close as possible to the blade tip.

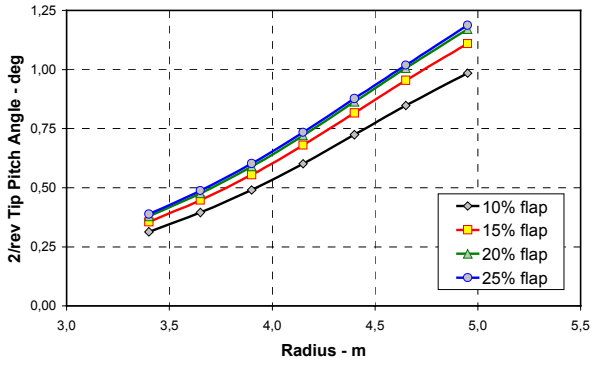

Fig. 2 2/rev pitch angle response at the blade tip due to a 2/rev flap amplitude of 5 deg as function of the radial flap position,
flap length 0.1R, hover case 3.5 t

Fig. 2 shows the blade tip pitch angle response caused by a flap motion with an amplitude of 5° at 2/rev, while the flap chord and the radial position was changed. Experience from former tests showed that the ability to suppress BVI noise is represented by this parameter. The response is clearly dominated by the servo effect. Increasing the chord above 15% of the blade chord does not improve the envisaged blade reaction significantly but increases the needed actuator power considerably. If there is a need, it is more effective to enlarge the radial extension of the flap.

Due to the blade tip design of the ATR with a swept back planform and the available actuation concept, the outboard end of the flap was limited to radius station 4.9 m (0.89R). Unfortunately, the most

beneficial location for vibration control is at the very tip or in the mid range span area as is demonstrated in Fig. 3. It shows the non-rotating 4/rev hub moment generated by a 3/rev flap motion with 5 deg amplitude as function of the radial flap position.

The reason for the poor response, when the center of the flap is positioned at approximately 4.6 m radius station (0.83R), is depicted in Fig. 4. For the cosine part of the 4/rev hub moment the lift and servo effect is shown separately. For the blade parameters taken, both effects have the same magnitude but opposite sign at that radius station. Yet not shown here the results for the other hub vibration loads are similar. Therefore, a placement at 4 m (0.73R) is preferable for vibration control.

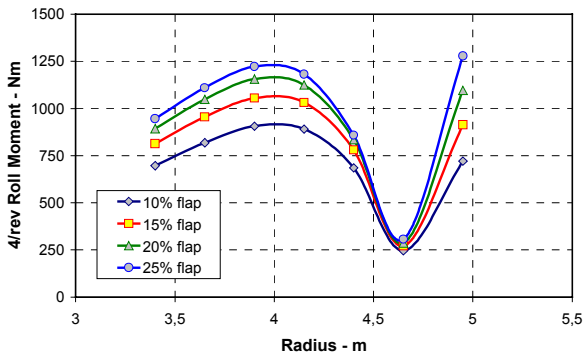

Fig. 3 4/rev hub moment response due to a 3/rev flap amplitude with 5 deg as function of the radial flap position,
flap length 0.1R, hover case 3.5 t

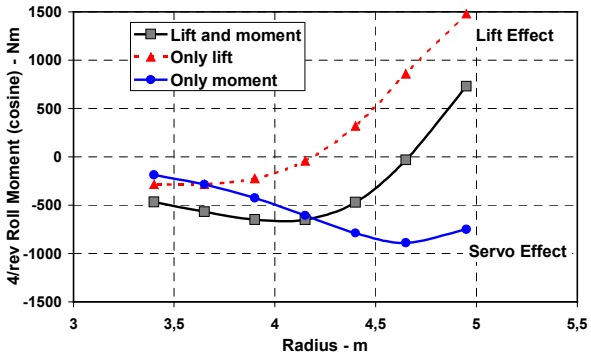

Fig. 4 Separation of lift and servo effect, 4/rev roll moment (cosine part) due to a 3/rev flap amplitude with 5 deg as function of the radial flap position, flap length 0.1R, hover case 3.5 t

In order to identify the influence of the aforementioned configurational parameters on noise and vibration control, ONERA and DLR performed dedicated analytical simulations [10], [12] based on the ECD rotor ATR (see Table 1). A representative result of attainable BVI noise reduction is depicted in Fig. 5. The maximum noise, for a descent slope between -6 and -8 deg, can be reduced by 5 to 7 dB(A). The outcome of the calculations confirmed the superiority of a small flap chord (15%) over a larger one (25%) under the desired limiting constraints.

The findings on BVI noise reduction could be confirmed and even exceeded by BO105 flight tests with Individual Blade Control through the blade roots (IBC). Even if this control mechanism differs from a flap control, the outer blade region behaves similarly to a flap controlled rotor. Hence a comparison appears realistic if the blade pitch amplitudes near the tip are similar.

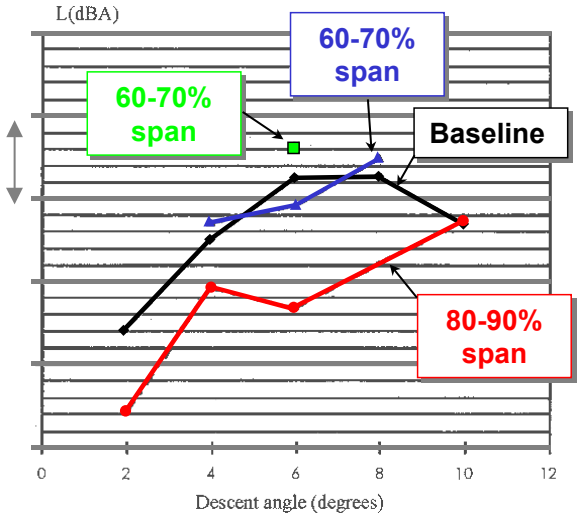

Fig. 5: Flap effect on BVI noise level

Actuators

Active Rotor Control requires high-performing and robust actuator technology. The flap actuator has to withstand high mechanical loads and should feature low volume and slim shape to fit into the blade section. The actuator should offer good electronic controllability and efficiency. During the design process of the flap control system, mainly two actuator candidates were investigated, the piezoceramic staple actuator with mechanical stroke amplification [11] and an electromagnetic device [13]. In spite of higher control amplitude and force of the electromagnetic actuator, the piezoceramic system was chosen. The reasons were the proof of the actuator's capability to sustain the centrifugal loads and its remaining inherent stiffness in case of a power loss.

Solid-state actuation technology based on active materials offers a new approach and within the group of active materials, piezoelectric ceramics (PZT) features a sufficiently high potential.

Piezoelectrical ceramic materials convert electrical energy directly into mechanical movement. The energy conversion takes place as soon as electrical energy is applied and is limited only by the dynamics of the mechanical system. Outstanding advantages of piezoelectrical actuators are their high dynamics, high deflection resolution, high force

generation, high specific working capacity and simple design.

Design and Dynamic Tuning

Rotor Blades

During the concept decision phase, the ATR rotor was the basis for the investigations. For the full scale rotor integration of the flaps, the blade of the EC145 was taken. It is aerodynamically identical to the ATR but features a fixed blade tip. The design of the blade was modified to integrate the active trailing edge flaps with characteristics as shown in Table 2. The whole flap system consists of three identical units with an individual length of 0.3 m. Dedicated studies showed that one pair of the available piezoelectric actuator is able to run a flap of 300 mm extension and a chord of 50 mm. The units can be installed at each of the three blade radial positions.

Table 2 Flap geometry

Chord	0.05 m, 15 %
Length	0.90 m, 0.16R
Radius station	3.8 - 4.7m
Unit 1	3.95 m, 0.718R
Unit 2	4.25 m, 0.773R
Unit 3	4.55 m, 0.827R
Max. flap angle	± 10 deg

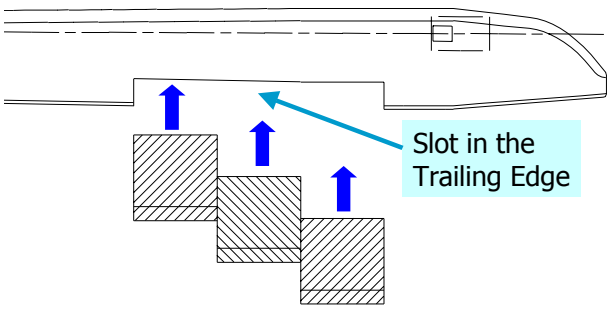

Fig. 6 Installation of the flap units from the trailing edge side

The design targets were as follows:

- Full integration in the existing blade geometry
- Low disturbance of the structural design
- Completely sealed against humidity
- The actuator/flap system should build a self-contained unit which could also be run outside the blade
- Easy mounting of the unit
- Low additional mass with most forward center of mass

For the implementation of the units the trailing edge of the blade was cut out (see Fig. 6) and the foam used as support between the upper and lower blade skin was substituted by a flat box made from carbon fiber. The box is open at the aft side. For obtaining an appropriate clearance during the insertion of the flap units the upper blade skin can be bend at the rear part as shown in Fig. 7. This approach avoids a big cut out. Finally, the parts are screwed and sealed to ensure the stiffness and strength requirements of the blade, as well as the protection of the flap actuation system against humidity.

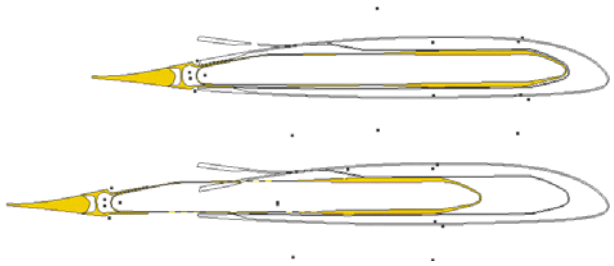

Fig. 7 Insertion of the flap unit into the blade

The result of highest interest for a successful application of flap control is the ability to induce an adequate hub load response for counteracting the rotor harmonic blade loads. It is well known that rotor harmonic airload excitations generally decrease with increasing harmonic number. In case of a four-bladed rotor, the 3/rev is the most important harmonic. To suppress BVI noise a 2/rev flap motion has been found to be most effective [1].

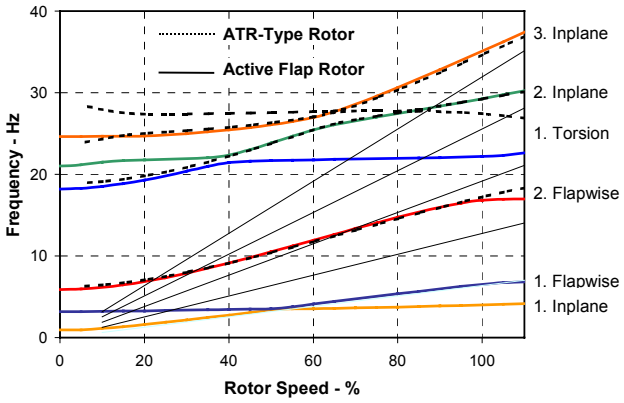

Fig. 8 Blade natural frequencies versus rotor speed calculated with CAMRAD II

Optimum response of the active flap occurs when the blade torsion frequency is near by the envisaged harmonics [14]. That is the reason why the torsion frequency of the blade was lowered in comparison to the reference blade of the EC145 (or ATR) rotor by substituting the carbon fiber in the blade skin inboard of the flaps by glass. The torsion frequency was tuned slightly below 3.5/rev. Fig. 8

shows the natural frequencies versus rotor speed for both configurations.

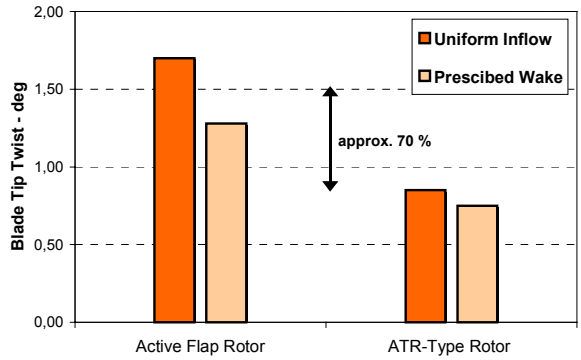

Fig. 9 Blade tip pitch angle due to a 5° flap input with 2/rev in hover condition (CAMRAD II)

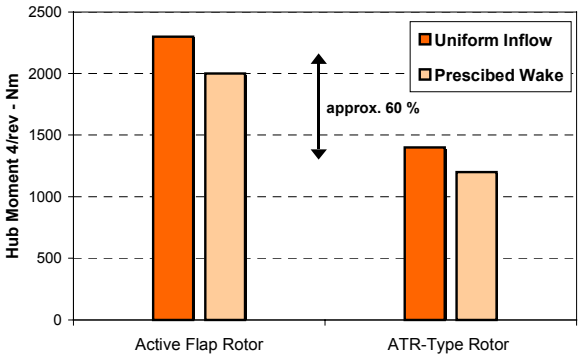

Fig. 10 Non-rotating hub moment due to a 5° flap input with 3/rev in hover condition (CAMRAD II)

Fig. 9 indicates a significant improvement of the 2/rev blade pitch response due to a 2/rev flap oscillation with 5° amplitude when the blade's torsion frequency is lowered from 4.9/rev to 3.4/rev. A similar result is found for a 3/rev flap oscillation which induces a 4/rev hub moment in the non rotating frame (see Fig. 10). The calculations are performed with CAMRAD II with an uniform inflow model and a prescribed wake model under axial flow conditions and at nominal rotor thrust of 35 kN. Calculations showed comparable results at forward flight conditions.

The main dynamic blade characteristics are given in Table 3. While the flap installation adds 4.5 kg at radius station 0.75R the tuning mass at 0.5R was reduced by about 2.5 kg. The lack of the standard pendulum absorber saves approximately 5 kg. Although the overall mass is reduced, the static moment is increased by 8% in comparison to the reference blade. The equivalent chordwise center of mass (weighted by radius) is shifted aft of the quarterline. This causes in combination with the decreased torsion frequency a stronger coupling with the flap bending modes (see Fig. 8).

Table 3 Dynamic blade characteristics (CAMRAD II)

Blade mass	42 kg
Static moment	120 kgm
Equiv. Center of mass	27.2%
Lock number	7.6
Equiv. Flap hinge offset	11.4%
Blade natural frequencies at nominal rotor speed	6.39 Hz
2nd flap	2.64/rev
3rd flap	5.5/rev
4th flap	8.7/rev
1st inplane	0.62/rev
2nd inplane	4.5/rev
1st torsion *)	3.4/rev

*) control stiffness not included

Flap Units

The actuator/flap unit is self-contained and can be run on bench outside the blade. Main data are shown in Table 4.

Table 4. Flap characteristics

Additional mass	4.5 kg *)
Flap mass, 0.9 m	0.27 kg
Control horn offset	3.5 mm
Frequency range	> 40 Hz

*) Based on two active units with 4 actuators and one dummy unit in comparison to the reference blade (ATR)

The most important design targets were:

- High structural stiffness
- Low friction of the bearings
- No mechanical play
- Aerodynamically sealed flap
- Low mass of the flap and the whole unit

One pair of piezoelectric actuators located at a most forward chordwise position act via tension rods on the flap (see Fig. 11). Losses caused by the elasticity of the load carrying structure are kept small by using carbon fiber for housing and tension rods.

At the rear edge of the carbon frame, a milled aluminum part is bonded which supports the flap bearings and the screwing to the blade. The flap itself is also made from aluminum and carbon fiber to keep the centrifugal and inertia forces as low as possible while the torsion stiffness is high.

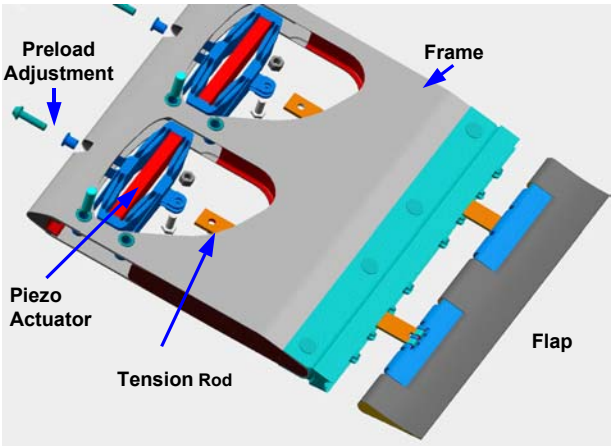

Fig. 11 Flap unit assembly

There are three types of bearings used. The flap motion is enabled by roller bearings, while the pull rods are connected to the flap with sliding contact bearings. The centrifugal forces are carried by the flap axle supported by a hard metal plate.

The arrangement of the piezoelectric actuators in the rotor blade is shown in Fig. 12. Within the first step of testing, two units will be active, whereas the third one is non-movable. If it is needed due to authority reasons it can easily be equipped with actuators.

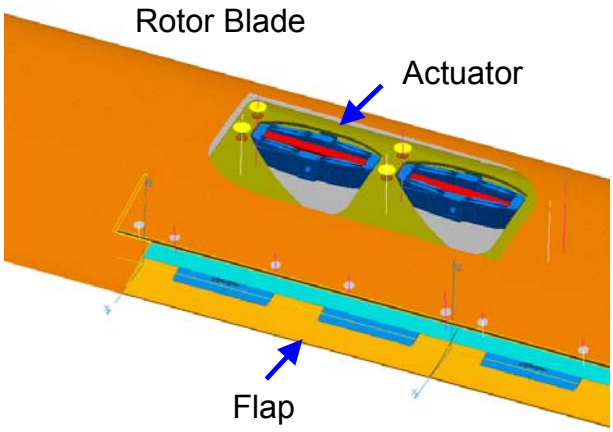

Fig. 12 Piezoelectric actuators embedded in the blade structure.

Power Electronics and Control

Powerful piezoelectric actuators as used in this application are a technical novelty which requires a new type of power supply and control. Laboratory test were performed with custom-made high power class-A amplifiers. Because this type of amplifier results into bulky design and additionally in poor power efficiency, an electronic concept suitable for flight vehicles was investigated. These investigations resulted in the development of switching-type amplifiers featuring a compact and lightweight design. A computer using a digital signal processor was used to implement a control system for coping with non-linearity, friction, external load and for surveying the power electronics.

Piezoelectric Actuator

Currently available piezoelectric ceramics materials provide little active strain in the order of 2000 microstrain. So-called monolithic co-fired multilayer stack actuators ("DWARF") fitting into the rotor blade generate a stroke in the order of 100 micrometer. Thus, a step-up gear is necessary to meet the stroke required for trailing edge flap actuation. The actuator system has to meet strict requirements:

- Gear ratio 1 : 10, gear output in chordwise direction
- Little height to stay within the blade cross section
- Small chordwise extension (most forward chordwise location)
- Stack orientation along the centrifugal field
- Stiff support of the piezostack and high gear stiffness
- No mechanical play, low friction
- Mechanical robustness
- Low weight and production-oriented design

In order to prevent play and wear, structural hinges were chosen. The efficiency of the gear was increased by the application of a multiple frame. The main characteristics are given in Table 5.

Table 5 Characteristics of one current available DWARF actuator

Blocking force	910 N
Blocking flap moment	± 1.6 Nm
Free stroke	1.45 mm
Maximum work	0.08 J
Voltage	600 V
Mass	400 g
Specific work	0.2 J/kg

Ceramic actuators need mechanical preload to avoid fracture. Using two actuators to move a flap provides this preload. While one actuator is pulling the second one is unloaded at the same time. This concept prevents any play but applies additional loads to the bearings of the flap (see Fig. 13).

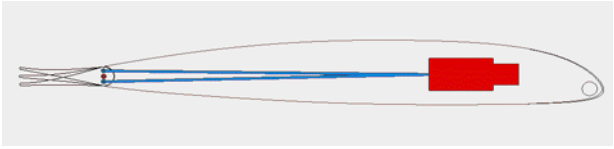

Fig. 13 Principle of flap control by the DWARF piezoelectric actuator.

Fabrication

After the design phase, the hardware for a full scale rotor was manufactured including:

- 4 airworthy blades fitting to the BK117 helicopter
- 1 blade for bench testing
- 15 actuator/flap units
- Several test specimens

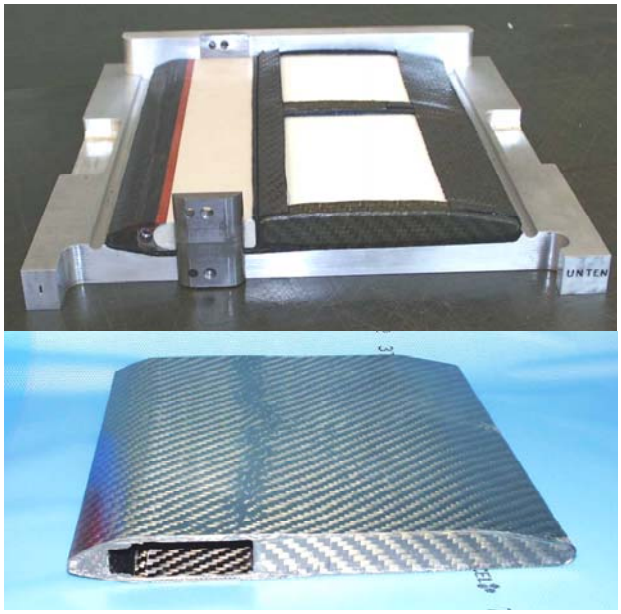

Fig. 14 Flap unit housing during manufacturing and after release from the mold

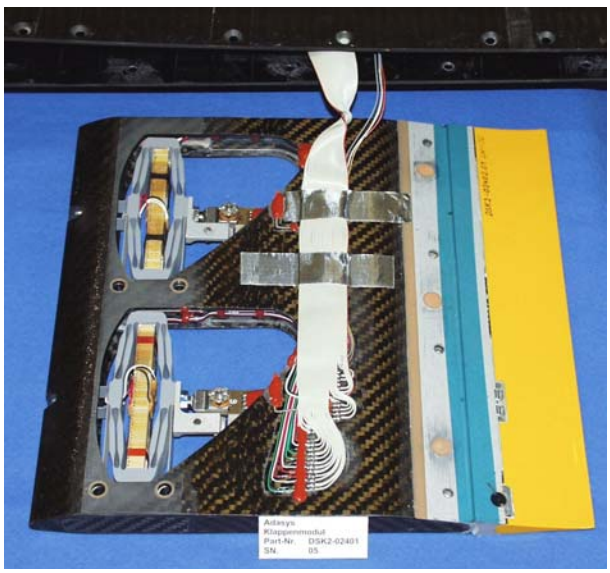

Fig. 15 Assembled flap unit with actuators

The existing moulds for the production blades of the EC145 were modified for the manufacturing process by additional tools to integrate the carbon box at the location of the flaps. For the installation of the wiring from the rotor hub to the piezoelectric actuators and to the sensors along the blade span, a groove was established in the blade surface along the quarterline.

Fig. 14 shows a flap unit housing during manufacturing and after release from the moulds before it undergoes further machining steps. A fully assembled unit is depicted in Fig. 15 just before it is inserted into to the blade, while Fig. 16 shows the finished blades with all the sensors and wiring ready for the test phase.

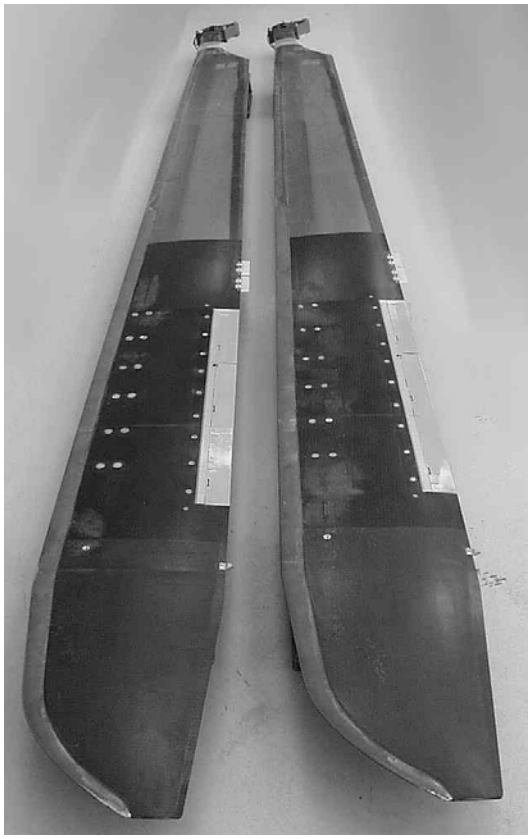

Fig. 16 BK 117/EC145 full scale rotor blades with integrated flaps and piezoelectric actuators.

Ground Testing

During the development process all main parts such as actuators, housing, flaps, tension rods, data pick-ups, wiring, power supply, and controllers had to undergo subsidiary test procedures.

Wind tunnel test

ECD and DLR performed tests in the Transonic Wind Tunnel, Göttingen with a non rotating full scale blade segment. It was equipped with four DWARF actuators which moved flaps with 0.5 m span in total [16, [17]. The main goals of the tests were to demonstrate the flap angles attainable under representative aerodynamic loads, to measure the lift, drag and pitch moments, and the pressure distribution by Kulite sensors, and to evaluate the servo effect of flap control.

Centrifugal test

For the qualification of the Dwarf actuator in the centrifugal field, a test with up to 800 g centrifugal load was run on a tail rotor test rig (see Fig. 17). It was powered and controlled via a conventional slip ring. No degradation of the power or strength problems due to centrifugal loads could be found.

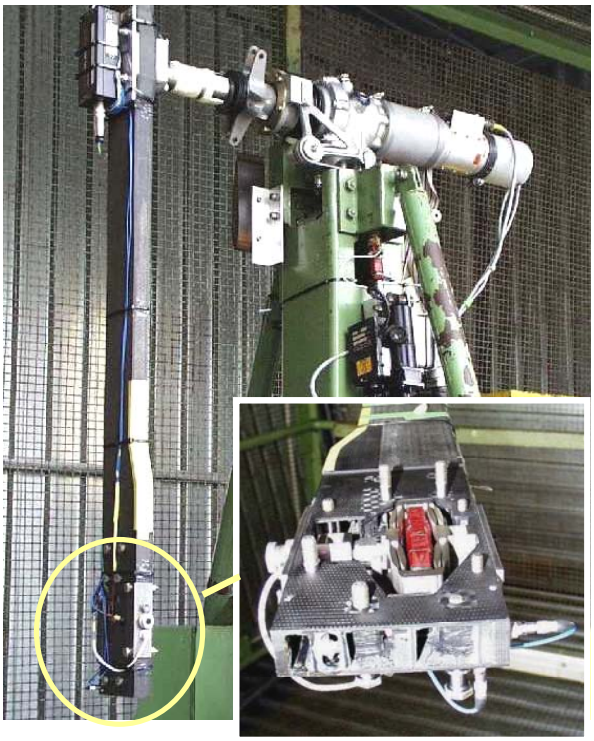

Fig. 17 Tail rotor test rig with DWARF actuator installed in the centrifugal test arm.

Bench tests

Mass and stiffness tests

An non-indented stiffness reduction of the load carrying parts can degrade the flap efficiency significantly. Therefore, tests should confirm the designed stiffness level. The longitudinal stiffness of a pull rod, the torsion stiffness of the flap, and the flap unit frame compressibility was measured. The results showed that the targets were reached and the losses were limited to about 10%. The mass penalty prevents a further stiffening.

A thorough evaluation of the mass, center of mass and moments of inertia of a flap unit as well as the test of the torsion stiffness of the blade was performed.

Endurance test of flap bearings

The bearings needed for the flap support are critical parts. Performance tests under realistic loads demonstrated an acceptable friction level and a life time adequate for an experimental system.

Actuators strength test

The verification of the robustness of the actuator flap system is an indispensable prerequisite before whirl tower and flight testing. The flexural hinges of the actuator frame and its fixings to the blade carrying the centrifugal load are regarded to be the most critical parts. A special test rig was built allowing biaxial loading of the actuators (Fig. 18). This is to simulate simultaneously aerodynamic as well as centrifugal loads. The specimen passed successfully tests applying first nominal operational loads and subsequently 50% overload condition.

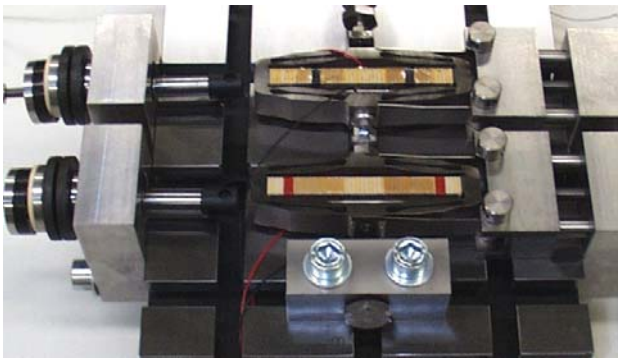

Fig. 18 Test rig for piezoelectric actuator endurce test

Actuator/flap unit system test

To assess the functionality of the actuator flap system including the control system tests simulating aerodynamic loads were carried out. External loads were generated by means of electromagnetic shakers. Fig. 19 shows one result of this testing. Clearly it can be seen how the control system eliminates the influence of the external forces as the flap angle curve features a sinusoidal signal as commanded.

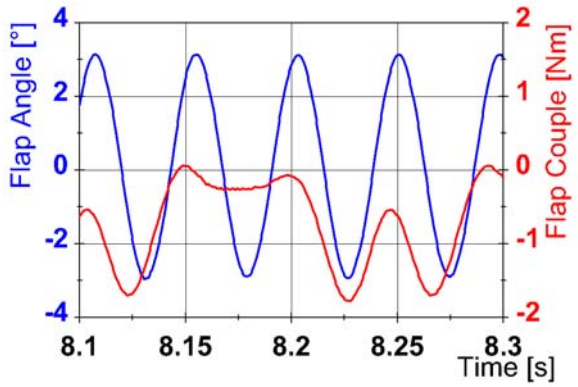

Fig. 19 Flap oscillation under simulated air loads in forward flight on the test rig

Dynamic tests

For the evaluation of the flap unit´s natural frequency, the actuators were run with a random noise voltage in the range of 1.25 and 500 Hz. Fig. 20 shows the transfer function indicating a natural frequency of approximately 200 Hz. This frequency is far above the working range.

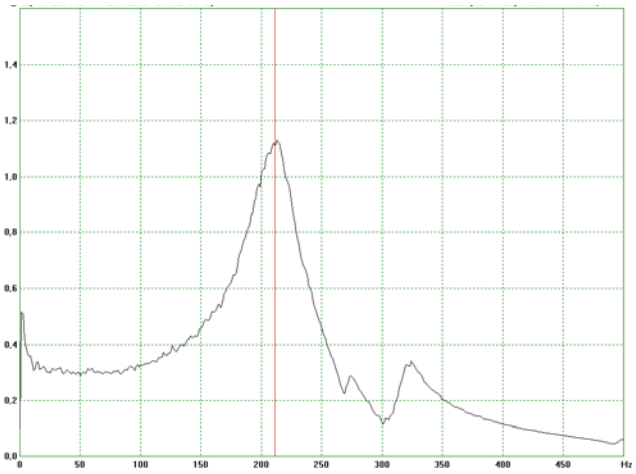

Fig. 20 Measurement of the natural frequency of one flap unit

Strength test of the blade

The segment of the blade containing the flaps was tested in a bending-machine shown in Fig. 21. While the specimen is clamped on the left hand side it is displaced on the opposite side. It survived the fatigue test over 500000 load cycles loaded with a level far above the flight limit loads. A final static overload test demonstrated the static strength capability of the blade structure. One active flap unit was operated during the tests to check a proper function even when the blade was bent in an extreme manner. A tension load of 10.7 kN simulating the centrifugal force at nominal rotor speed was superimposed on bending and torsion moments.

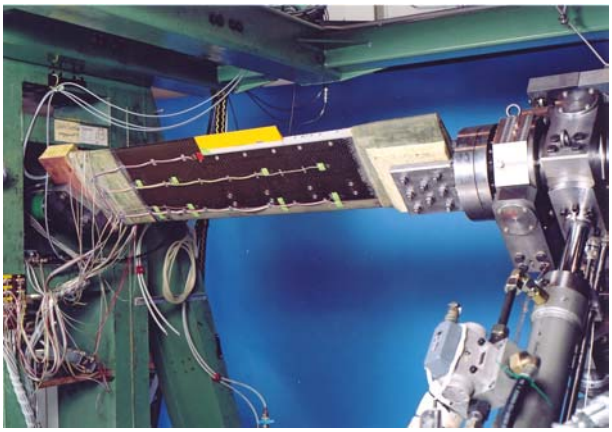

Fig. 21 Blade specimen with active flap during fatigue test

Whirl Tower Test

Test stand

The whirl tower depicted in Fig. 22 is a test facility for helicopter rotors up to a 70 kN thrust level. Table 6 comprises the main characteristics. The test and control equipment allows the tracking and balancing of the blades as well as the measurement of the thrust and performance characteristics. A three axes excitation system in the fixed frame gives the opportunity to evaluate aeroelastic properties of rotors such as natural frequencies and lead-lag damping. While a conventional slip ring is used for supplying the piezoelectric actuators, the rotor monitoring signals are transmitted by a telemetry system with 40 channels.

Fig. 22 ECD test stand for main rotors

Table 6 Whirl tower main characteristics

Dimensions:	
Rotor altitude	6.6 m
Max. diameter	13.5 m
Drive unit:	
Direct drive DC motor	1230 kW
Maximum torque	45 Nm
Sense of rotation	bidirectional
Max. speed	450 rpm
Swash plate controls:	
Frequency range	48 Hz
Test equipment	
Telemetry system	40 channels

Test specimen and setup

For time and complexity reasons, only one blade pair was run during the first test campaign. Fig. 23 and Fig. 24 show the blades mounted at the whirl tower. The mid position of the three units at each blade was active. Table 7 summarizes the signals monitored.

Fig. 23 Flap rotor blade on the Whirl tower

Table 7 Signals available during the Whirl tower test

Rotor thrust and torque	
Mast bending moment	
Pitch link forces	
Booster loads	
Flap bending moments	R= 0.522m
Lead-lag bending moments	R= 0.672 m
Pull rod forces	
Actuator displacement	
Flap inclination	
Actuator voltage	
Temperature of Piezo stack	
Track attitude	R= 4.6 m

Fig. 24 BK117 hingeless rotor hub with signal processing electronics on the whirl tower

Baseline test matrix

The goal of the initial test phase on the whirl tower was to evaluate the aeroelastic properties of the blades such as natural frequencies and inplane damping as well as the capabilities of the active flap units.

Most of the tests were conducted at nominal rotor speed with collective pitch settings up to 8 deg. At first, the flaps were deflected with steady inclination to check the flap´s influence on the blade track and blade control forces. During the dynamic tests the flaps were run at various flap angle amplitudes with frequencies up to the sixth rotor harmonic. The deflection was commanded both by rotor harmonics and by further pure sinusoidal flap control inputs.

The reaction of the flap without power supply was studied in the available thrust range. Finally a sweep up to 50 Hz should confirm the natural frequency measurements already performed with the whirl tower excitation system.

Test results

Fig. 25 shows the test results gained by the aforementioned method at nominal rotor speed as well as for the rotor at rest. The data found fit well to the coupled natural frequencies calculated by the CAMRAD II code.

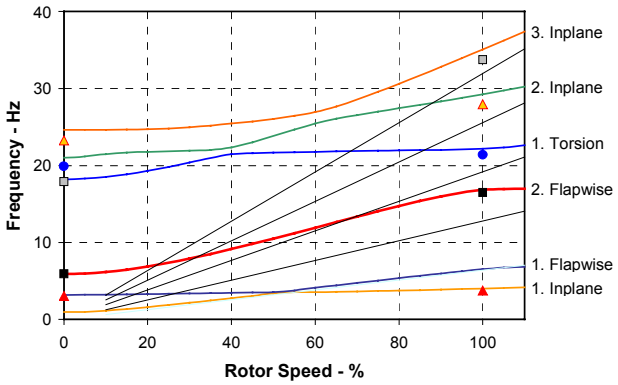

Fig. 25 Comparison of the tested blade natural frequencies (symbols) with calculation (CAMRAD II).

Table 8 Sign conventions

Blade flaps up	Positive flap angle
Trailing edge flaps moves upward	Negative inclination angle
Blade pitches nose down	Positive pitch link force

The reaction of the blade track attitude, when the trailing edge flap is inclined, is shown in Fig. 26. For sign convention see Table 8. When the center flap (0.773R, 300 mm length, 50 mm chord) is inclined by 5° the blade flap angle changes by 0.25° equivalent to 21 mm displacement at the blade tip.

This is equivalent to a thrust change of 900 N or 10% of 1g thrust. The effect on the blade control force is depicted in Fig. 27. It is increased by 250 N which is equal to a pitch moment of 41 Nm.

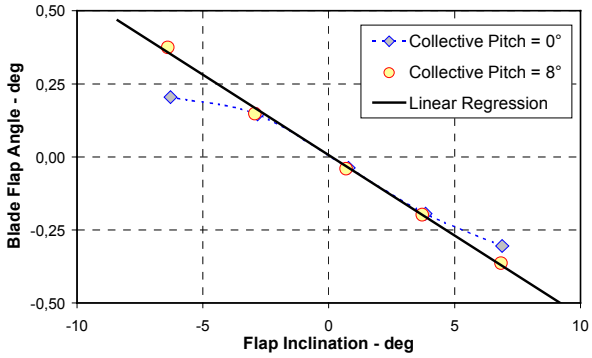

Fig. 26 Variation of blade track due to a steady flap inclination (0.773R, length 0.3 m)

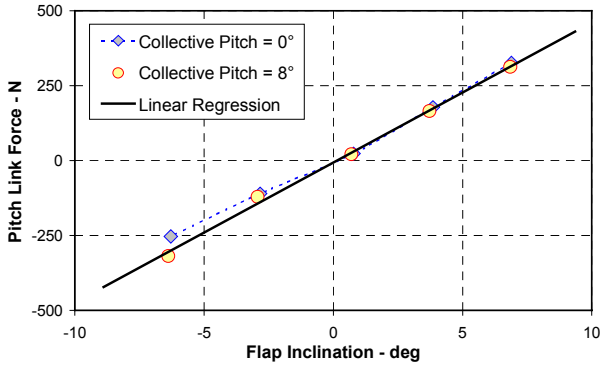

Fig. 27 Variation of blade control force due to a steady flap inclination (0.773R, length 0.3 m)

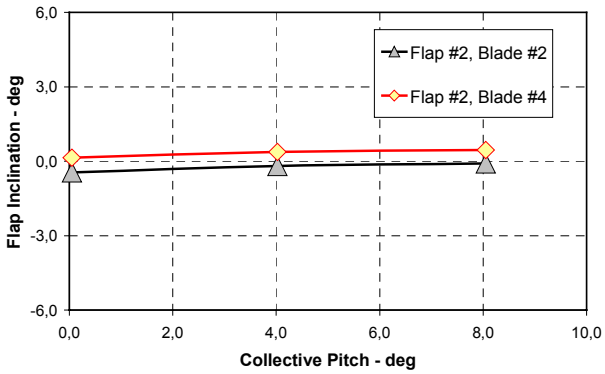

Fig. 28 Flap inclination with power supply switched off versus collective pitch setting at nominal rotor speed

When the power supply of the actuators is switched off the flap is positioned by the balance of the actuator stiffness and the external air loads. Fig. 28 shows the results versus collective pitch setting. In the range tested the flap angle in nearly independed from the angle of attack of the profile. It is well centered by the implementation of a pre-inclination flap angle of -3 deg. Fig. 29 shows the unfiltered time history in addition with the corresponding actuator voltage for a 3/rev excitation with an amplitude of 5 deg.

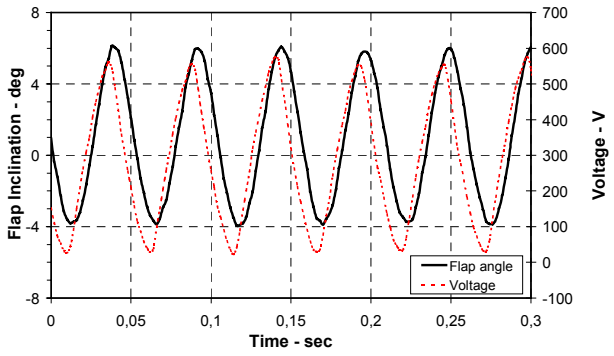

Fig. 29 Time history of flap inclination and actuator voltage during a controlled 3/rev flap actuation, collective pitch setting 8°

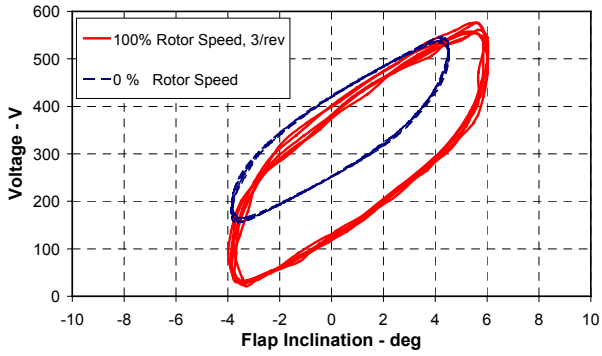

Fig. 30 Actuator voltage versus flap inclination angle. Time history of a 3/rev flap oscillation.

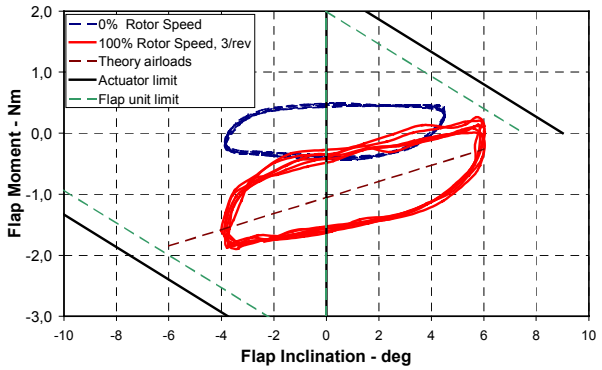

Fig. 31 Flap moment versus flap inclination angle. Actuator capabilities and time history of a 3/rev flap oscillation at 5 deg amplitude.

Fig. 30 depicts the actuator voltage and Fig. 31 the flap hinge moment versus the flap inclination. The latter is derived from the pull rod forces measured by strain gauges. The hysteresis indicates the friction mainly caused by the pull rod bearings. The limits given by the current piezoelectric actuator

technology are indicated too. The performance compared to the isolated actuator is slightly diminished by the flap unit stiffness.

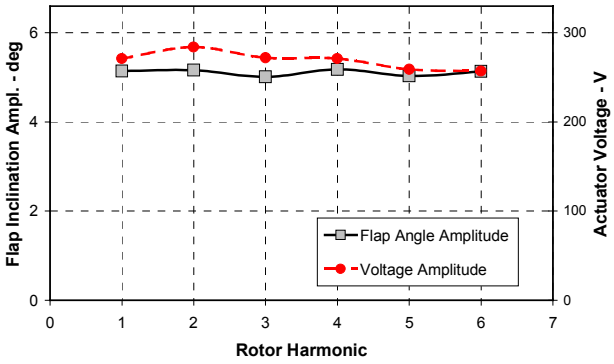

Fig. 32 Flap inclination and voltage amplitude versus actuation frequency, collective pitch setting 8°

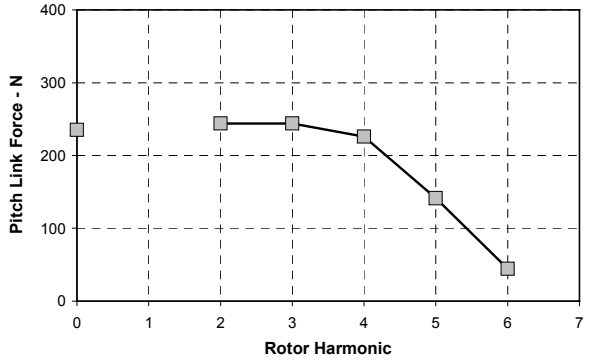

Fig. 33 Pitch link force amplitude at the appropriate flap oscillation frequency, amplitude 5 deg

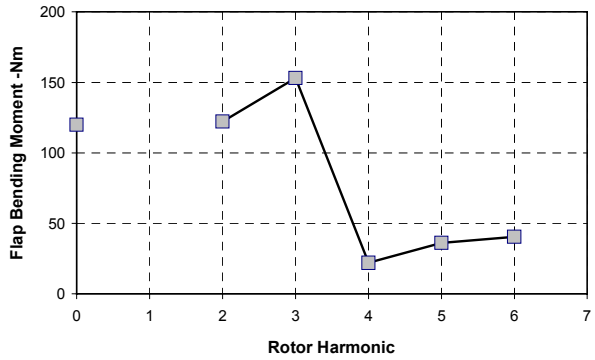

Fig. 34 Flap bending moment amplitude (r= 522 mm) at the appropriate flap oscillation frequency, amplitude 5 deg

The flap excitation frequency was increased step by step from the first rotor harmonic up to the sixth harmonic. Test results confirmed that the applied voltage amplitude remains approximately the same when the flap amplitude is kept constant (see Fig. 32). But the blade response decreases significantly, as is documented in Fig. 33 for the pitch link force and in Fig. 34 for the blade flap bending moment measured at radius station 522 mm (0.095R). The 1/rev data are not shown because of perturbations by wind.

During the test phase the rotor was run for 10 hours. Most of the time, the actuators were switched on. No mechanical or electrical problems occured.

Planed Flight Testing

System architecture

A sketch of the equipment to be installed in the BK117 test helicopter is shown in Fig. 35.

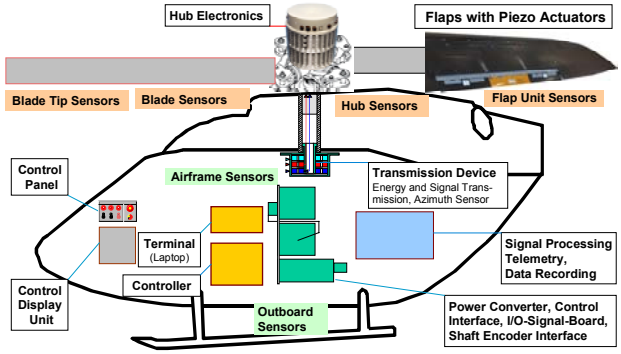

Fig. 35 System architecture of the test helicopter

Besides the rotor with active flaps and the appropriate sensors, a cylindrical compartment is mounted on the rotor hub (Fig. 36). It houses the signal conditioning and processing as well as the power distribution to the individual flap units.

Fig. 36 Hub electronic compartment during a test installation on the helicopter

The airframe contains:

- Power converter
- Control interface
- I/O-signal-board
- Shaft encoder interface
- Control computer with terminal
- Data recording and telemetry devices

For the transfer of the electric power, a brushless transducer is installed below the gear box. The electric connection to the hub is established by a coaxial metal tube with a diameter of 8 mm. It contains additionally two plastic fibers which are used for the optical data link in both directions.

Monitoring

Each blade is equipped with sensors and the corresponding wiring along the blade span. The following parameters are measured:

- Actuator forces and strokes
- Flap angles
- Accelerations at hub and blade tip
- Pressure (Kulite)
- Structure born sound of vortex impingements
- Temperatures in the flap unit
- Blade bending and torsion moments
- Control forces
- Fixed system sensors: microphones, accelerations, control loads, control angles,...)

Most of sensors are standard gauges but some are especially adapted to the environment or task, like the sensors for flap angles and actuator stroke.

For BVI detection a new sensor type based on a piezo film is used. It has the capability to sense the structure born sound in the rotor blade which is generated when a vortex hits the blade surface. Because it is applied at the inner side of the metal erosion strip the sensor is very robust. The location is at radius station 0.8R [1].

Failure analysis

The system is completely independent from the primary flight control and it is not a flight safety critical item. In case of mal function or loss of electric power of the actuation system an uncomfortable vibration level may appear but it will not influence the controllability and safety of the helicopter.

EMC

The additional electric equipment runs the risk to encounter EMC problems in the helicopter. There are a middle frequency brush-less electric transducer and some switching amplifiers on board as well as computers for the controlling and the data transfer between rotating and non-rotating frame. Low level voltage of the data acquisition has to be handled in the neighborhood of high voltage with steep slew rates. Therefore, high emphasis is given to these effects which will be thoroughly tested during the ground test phase.

Flight test envelope

After the ground runs, a flight test program will be carried out to evaluate the function of the flap system within open loop and closed loop tests. The goal is to demonstrate the efficiency of Active Blade Control by flaps with respect to different control goals.

Controller and control laws

Due to the high unsteadiness of a typical helicopter flight, fast control loops are required to achieve satisfying results in noise and vibration reduction. This is best accomplished by using control algorithms in the time domain. However such systems require a reliable analytical model of plant and actuator in order to be properly designed. Since this represents a demanding postulation particularly for noise reduction, first investigations have been performed already with a relatively simple controller based on frequency domain.

The 2/rev differential mode used for these trials has been successfully tested in open loop configuration on a BO105 rotor, equipped with the ZFL IBC system, both in the NASA Ames 40 by 80 ft wind tunnel [4] and in flight tests at ECD [3].

Efficient vibration reduction has been demonstrated by application of Higher Harmonic Control – HHC (by actuators in the fixed system). This was done by flight tests at Aérospatiale, now EC [18], and by wind tunnel tests in the DNW with a Mach-scaled 4 m diameter BO105 model rotor [4]. It was also confirmed by open loop BO105 flight tests with the IBC system. Now, closed loop tests with this system will follow. The envisaged time domain controller has been developed at ECD [1]. It is based on a Notch filter centered on the 4/rev rotor signal. As control harmonics 3/rev, 4/rev and 5/rev signals will be applied corresponding to collective, lateral and longitudinal blade pitch modes.

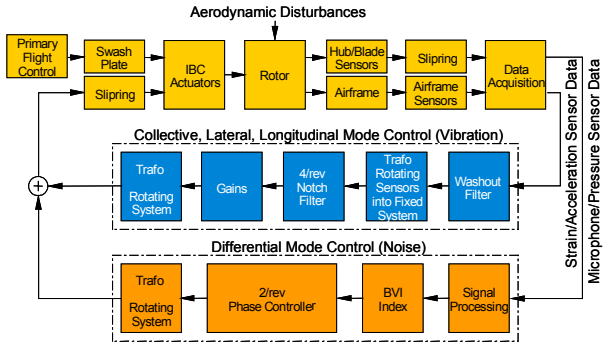

Fig. 37 Controller architecture for simultaneous BVI noise and vibration control

The separation of the control frequencies for noise (2/rev) and vibration (3-,4-,5/rev) reduction appears necessary, since the HHC tests showed that simultaneous noise and vibration reduction only by 3/rev, 4/rev and 5/rev was impossible. The two control tasks are now to be accomplished by one controller with two different feed back loops (see Fig. 37). The control algorithms developed with the aid of the IBC tests on BO105 will afterwards be transferred to the flap control on BK117. This appears possible, since the outer blade region behaves similarly for both control strategies.

Conclusions

Active Blade Control is the only technology to reduce exterior noise and cabin vibrations at the same time and with the same system. Development and successful testing of this control system based on small piezoelectric driven trailing edge flaps has been described above.

The results attained during tests on a spin rig, on a blade component test stand, and finally on a whirl tower demonstrate that the control system is able to work reliably under the demanding boundary conditions of high centrifugal and blade bending loads.

In particular, the ruggedness of actuation system and flap unit suspension in the blade, as well as the attainment of the expected flap inclination angles proved the operability of the control system.

Hence, the technology of Active Blade Control by trailing edge flaps is ready for flight testing.

Acknowledgements

This work was supported by the German Ministry of Economics (BMWi) within the research program ADASYS II. The authors would like to thank the colleagues of EC-SAS, ONERA and DLR for the parametric and optimization studies during the concept phase.

References

[1] Roth D., Dieterich O., Bebesel M., Pongratz R., Kube R., Munser H., "Individual blade root control demonstration - recent activities", 27th European Rotorcraft Forum in Moscow, Russia, September 2001

[2] Straub F., Hassan A., "Aeromechanic Considerations in the Design with Smart Material Actuated Trailing Edge Flaps", 52nd AHS Annual Forum, Washington, DC, June 1996

[3] Teves, D., Kloeppel, V., Richter, P., "Development of Active Control Technology in the Rotating System, Flight Testing and Theoretical Results", 18th European Rotorcraft Forum, Avignon, France, 1992

[4] Jacklin, S.A., Blaas A., Teves, D., Kube, R., "Reduction of Helicopter BVI Noise, Vibration and Power Consumption through Individual Blade Control", 51st Annual Forum of the American Helicopter Society, Ft Worth, 1995

[5] Dieterich, O., "Application of Modern Control Technology for Advanced IBC Systems", 24th European Rotorcraft Forum, Marseille, France, September 1998

[6] Friedmann P., "The Promise of Adaptative Materials for Alleviating Aeroelactic Problems and Some Concerns", RAE Conference "Innovation in Rotorcraft Technology", London, UK, June 1997

[7] Chopra I., "Status of Application of Smart Structures Technology to Rotorcraft Systems", RAE Conference "Innovation in Rotorcraft Technology", London, June 1997 (republished in Journal of the AHS Society, Vol. 45 (4), pp 228-252, October 2000)

[8] Hasegawa Y., Katayama N., Kobiki N., Nakasato E., Yamakawa E., Okawa H., „Experimental and Analytical Results of Whirl Tower Test of ATIC Full Scale Rotor System", 57th Annual Forum, Washington, DC, May 9-11, 2001

[9] Bebesel M., Schoell E., Polz G., "Aerodynamic and Aeroacoustic Layout of ATR (Advanced Technology Rotor)", 55th AHS Annual Forum, Montreal, Canada, May 1999

[10] Leconte P., Kube R., "Main Rotor Active Flaps: Numerical Assessment of Noise and Vibration Reduction", 2nd ONERA-DLR Aerospace Symposium, Berlin, June 2000

[11] Jänker P., Hermle F., Lorkowski T., Storm S., Christmann M., Wettemann M., Klöppel V., "Development and Evaluation of Advanced Flap Control Technology Utilizing Piezoelectric Actuators", 25th European Rotorcraft Forum, Rome, September 1999

[12] Leconte P., Rapin M., Van der Wall B.G., "Main Rotor Active Flaps: Numerical Assessment of Vibration Reduction", 57th AHS Annual Forum, Washingtion DC, May 2001

[13] Toulmay F., Klöppel V., Lorin F., Enenkl B., Gaffiero J., "Active Blade Flaps – The Needs and Current Capabilities" , 57th Annual Forum, Washington, DC, May 9-11, 2001

[14] Ormiston R. "Aeroelastic and Dynamic Rotor Response with On-blade Elevon Control", 24th European Rotorcraft Forum, Marseille, France, September 1998

[15] Straub F., Charles B., "Comprehensive Modeling of Rotors with Trailing Edge Flaps", 55th AHS Annual Forum, Montreal, Canada, May 1999

[16] Schimke D., Jänker P., Wendt V., Junker B., "Wind Tunnel Evaluation of a Full Scale Piezoelectric Flap Control Unit", 24th European Rotorcraft Forum, Marseilles, September 1998

[17] Schimke, D., Jänker, P., Blaas, A., Kube, R., Schewe, G., Keßler, C., "Individual Blade Control by Servo-Flap and Blade Root Control – A Collaborative Research and Development Programme", 23rd European Rotorcraft Forum, Dresden, Germany, September 1997

[18] Achache M., Polychroniadis M., "Development of an Experimental System for Active Control of Vibrations of Helicopters", 12th European Rotorcraft Forum, Garmisch-Partenkirchen, 1986